Journal of Nuclear Materials 401 (2010) 104–112

Contents lists available at ScienceDirect

Journal of Nuclear Materials

journal homepage: www.elsevier.com/locate/jnucmat

Effect of the synthesis method on the properties of a Pb-bearing (Y–Gd–Ce) rare-earth phosphate used for the confinement of high-level radioactive waste

Nour-el-hayet Kamel [a,*], Khadoudja Remil [a], Malika Arabi [a], Ziane Kamel [a], Ahmed Zahri [a], Samia Metahri [b]

[a] Algiers Nuclear Research Centre, Division of Nuclear Techniques, 2 Bd Frantz Fanon, P.O. Box 399, Algiers RP, Algeria
[b] Algiers Nuclear Research Centre, Division of Environment, Radiological Safety and Radioactive Waste, 2 Bd Frantz Fanon, P.O. Box 399, Algiers RP, Algeria

ARTICLE INFO

Article history:
Received 12 July 2009
Accepted 10 April 2010

ABSTRACT

In this study, a Pb-containing (Y–Gd–Ce) rare-earth phosphate with the general chemical formula of $(Y_{0.1}Pb_{0.1}Ce_{0.4}Gd_{0.4})PO_4$ was synthesized by two methods, namely the sol–gel and the metallurgical method. The sol–gel route consists of an external gel precipitation method, followed by two calcinations at 873 and 1473 K; and the dry route was a natural sintering at 1473 K of a mixture of micropowders activated at 873 K. The sol–gel route of synthesis gives a stronger and harder monazite mineral than the one obtained by the dry route of synthesis, both of them have a very low porosity. The sintering densities are 4.70 and 4.55 g/cm^3 for both the sol–gel and dry-route made monazites. The X-ray diffraction (XRD) analysis shows a main monoclinic crystalline structure for the two ways of synthesis. However, a secondary anorthic phosphate phase appears for the dry-route made monazite. Three leaching tests simulating several radiological events were performed: an acidic static test at different pH, a static water leach test in an argilous media and a dynamic microwave leach test.

For the whole of leaching processes, the kinetic of dissolution is fast. The acidic tests at pH 1, 4 and 7 gave few amounts of dissolved Ce in the leachates, about 5.668, 0.189 and 0.346×10^{-2} g/m^2 day at the steady-state, respectively. The Pb was totally dissolved at pH 1 and 3. The sol–gel made monazite has a weak chemical durability in acidic media. In neutral pH, both the sol–gel and the dry-route made monazites give comparable values of Ce normalized dissolution rates (0.346×10^{-2} and 0.389×10^{-2} g/m^2 day, respectively). The leaching in kaolin media decreases with a ten factor the amounts of leached Ce. However, for the whole of the leaching tests performed in neutral pH conditions, the monazite materials have a good chemical durability. The dissolution of the minerals under the microwave leaching is partially achieved, with only 3.5% and 4.0% of solubilised minerals, for both the sol–gel and dry-route made monazites, respectively, showing the good chemical durability of the studied monazite mineral.

1. Introduction

The monazite mineral is a ceric-earth orthophosphate with little amounts of yttric-earths and variable amounts of thorium (Th). Rare-earth phosphates have the general chemical formula of $LnPO_4$, nH_2O (where Ln may be a lanthanide or an actinide (An) or yttrium (Y)). They may contain little amounts of bivalent cations, like Ca, Ba, Sr, Cd or Pb [1]. The bivalent cations allow reaching the tetravalent state of Ln and An in the structure, except Am which never forms the tetravalent state into the monazite structure [2,3]. The behavior of the other actinides when incorporated in phosphate ceramics is quite similar each other. It is important to note that Cm and also Am are better stabilized in the trivalent oxidation state, as reported by Dacheux et al. [4].

However, depending on the synthesis methods and conditions, one can find the monazite chemical forms of: $Ln(PO_3)_3$, $Ln(PO_3)_4$, $Ln(PO_4)_2$ or $Ln_2P_2O_7$ [3–8]. These actinides-bearing minerals are chemically and crystallographically stable even after hundreds of years [5–7]. For this, there are extensively studied as natural analogues in the field of minor actinides immobilization.

In a geological point of view, the mineral compound $LnPO_4$ exists since several millions of years. One can enumerate more than 300 natural mineral phosphates, which are classified in several groups [8]. The monazite phosphates, $LnPO_4$, constitute the main Th ore and are a significant source of rare-earth elements in the earth crust [9]. There are located in pegmatites, syenites, diorites and in the derivative metamorphic formations of these rocks (gneiss, etc.). Also, there are present in river sands and sea coastal beaches resulting from granitic rocks erosion alterations [10]. The most known anhydrous orthophosphates are the two solid solutions monazite/cheralite or monazite/brabantite, recently renamed as monazite/cheralite, according to the CNMMN nomenclature,

* Corresponding author. Tel.: +213 21 43 44 44; fax: +213 21 43 35 38.
E-mail address: benhabiles.kamel@yahoo.fr (N. Kamel).

0022-3115/$ - see front matter © 2010 Elsevier B.V. All rights reserved.
doi:10.1016/j.jnucmat.2010.04.005

and monazite/xenotime [11]. Besides these, three hydrated forms of $LnPO_4$ exist, from which two are also known as natural minerals: the rhabdophane and weinschenkite or churchite [12].

Monazites minerals belong to geological chains which have excellent An uptakes, and are very stable. Very abundant literature relates the hydrogeological behavior of many natural analogues in presence of kaolin clays or granitic rocks. In particular, the dissolution of actinides elements is inhibited in hydrological media nearest the kaolinite mineral. This characteristic is used to study the possibility to use natural analogues (monazite, perovskyte, pyrochlore, zirconolite, etc.) as confinement materials in clayey undergrounds [13–20].

Two major ways of synthesis are employed to fabricate monazite minerals: the wet and dry synthesis. The first one is a solid-state synthesis. It may start from mixtures of Ln oxides, nitrates or carbonates and hydrogen phosphates, with one or successive grinding/high-temperature calcination steps [21]. The calcination may be a classical sintering, a firing, a flux-growth method, etc. [22–26].

When starting from an oxide free mixture, many wet monazite synthesis methods exist. In sol–gel reactions, the reagents are dissolved in water or nitric acid solutions, and then are transformed in xerogels. The gels are calcinated, grinded and sintered to form the final phosphate product [1,27]. Other hydrothermal synthesis methods use long heating steps at low temperatures (150–400 °C) in closed reactors. These syntheses are conducted in sand baths or autoclaves [28,29].

The chemical durability of synthetic monazites is scarcely studied [21]. However, Terra research team has reported significant data on the leaching of these actinides sequestration matrices [28–34]. It is well known that the durability of the crystalline structure of synthetic monazites depends on two opposite effects: the creation of structural defects and the self-annealing at relatively low temperature [35]. It is a function of the activity of the radionuclide contained in the mineral, its specific decay period and its incorporation rate.

In the literature, several studies treat of the characteristics of synthetic natural analogues as monazites, britholites and pyrochlores [16,28,29,35–38].

In this paper, we were interesting in a lanthanide phosphate of general formula: $(Y_{0.1}Pb_{0.1}Ce_{0.4}Gd_{0.4})PO_4$. This chemical composition was chosen based on bibliographic data. Thus, lead (Pb) was added as a bivalent cation. It permits reaching the tetravalent state of Ln added cations. Yttrium (Y) replaces a lanthanide. Gadolinium (Gd) is a particular lanthanide with a large neutron capture section, and cerium (Ce) is an actinide surrogate (Th, U, etc.).

The mineral is synthesized with both a sol–gel and a powder metallurgical method. With the aim of comparing the efficiency of the two synthesis processes, the two obtained synthesis products are characterized by their densities; crystalline structure, porosity, hardness and three leaching tests: an acidic static test at different pH, a static water leach test in an argilous media, and a non-conventional microwave leach test [39]. The leach test in an argilous media is used to study the behavior of this monazite mineral in the case of a water infiltration in a clayey waste repository.

2. Experimental

The dry synthesis was made following Montel et al. method [1]. The chemical reagent are the commercial products: Y_2O_3 and CeO_2, (Aldrich, 99.999%), PbO (Merck), $GdCl_3\ nH_2O$ (Cerac), $(NH_4)_2HPO_4$ (Fluka p.a., >99%). The gadolinium chloride was first calcinated three times at 1613 K during 12 h in order to transform the chloride salt in oxide. Both the rates of heating and cooling were of 20 and 15 deg/min, respectively. The calcinations as well as the other heat treatments performed in this study were conducted in a Carbolite furnace RHF 1600. X-ray diffraction (XRD) analyses confirmed the gadolinium oxide formation (JCPDS pattern number 00-042-1465 from JCPDS data [40]). The diammonium phosphate and all the metal oxides were separately crushed 10 min in an automatic agata mortar Controlab N6 87–60 K, then milled manually in an agata mortar, in order to obtain micropowders with grain sizes lower than 28 μm. The monazite mixture was prepared in stoechiometric proportions so that the final chemical product has the chemical formula of: $(Y_{0.1}Pb_{0.1}Ce_{0.4}Gd_{0.4})PO_4$. About 4% of zinc stearate was added as an organic lubricant. The mixture was homogenized for 8 h in an adapted Controlab D403 shaker. It was calcinated at 873 K during 24 h. Both the rates of heating and cooling were: 25 and 15 deg/min, respectively. This supplementary calcination step was added to eliminate the organic and nitrified compounds before the compaction in pellets, which will lead to a compact final product. Pellets of 13 mm of diameter with various heights were prepared by uniaxial compaction in a Sodemi RD 20 DE press, at an average pressure of 240 MPa. The pellets were first dried overnight in a steam room at 353 K, then sintered in air at 1473 K for 24 h, with a thermal cycle such that: both the rates of heating and cooling were 25 and 15 deg/min, respectively.

The dry synthesis was made following Gardes et al. method [23]. The sol–gel synthesis was conducted using the metallic nitrates salts: $Ce(NO_3)_3{\cdot}6H_2O$ (Acros Organics, 99.5%), $Y(NO_3)_3{\cdot}6H_2O$ (Acros Organics, 99.9%), Gd $(NO_3)_3{\cdot}6H_2O$ (Aldrich, 99.99%), $Pb(NO_3)_2$ (Merck, 99.5%), dissolved in nitric acid (Fluka, p.a.) under a strong stirring at the temperature of 353 K. The gel formation occurs with adding an ammonia solution (Merck p.a., 25%) to the salts bath which contains organic emulsifiers (Urea, HMTA, Aldrich) under a strong stirring. The gel was washed 72 h with ultra-pur water (Aldrich) on glass filters until the pH decreases to the value of 8.5. It was dried one night at 353 K, and calcinated and sintered following the same procedure used for the dry route of synthesis. Also, the calcination step was added to eliminate the organic and nitrified compounds before compaction, which leads to a compact sintered product.

The materials densities, before (d_g) and after (d_s) sintering, were measured by the geometrical method. Phase identification of the materials was done by XRD analysis with a monochromatic Cu Kα Philips X'Pert Pro diffractometer, using Philips X'Pert High Score software [40]. Both grains and pores distribution of the matrices was performed with a scanning electron microscope (SEM): Philips XL 30, equipped with an EDX, ESEM-FEG probe.

Specific area measurements were made using a sorption/desorption BET Asap 2010, with nitrogen gas at 77 K. Vickers indentations were measured using a 368–372 Reichert-Austria apparatus, equipped with a 68–309.1 Reichert-Austria camera.

Three corrosion tests were performed on the synthesized mineral: an acidic water static leach test at several pHs (1, 4 and 7), a static leach test simulating the long-term geological disposal conditions, performed in kaolin containers; and a non-conventional microwave leach test. This last is a dissolution test in highly aggressive conditions. These kind of non-standard techniques are used to improve the dissolution of specific ceramics under severe leaching conditions [39].

The static leaching tests were performed either in dark closed glass vials or in kaolin containers. The water leach test (kaolin free) was performed at starting leachate pHs of 1, 4 and 7, in HCl (Merck p.a.) diluted solutions. Either for the long-term geological disposal test or for the neutral water leach test, the leachates of pH 7 consist on bidistilled water.

The kaolin containers were fabricated using a pure kaolin ore originated from Djebel Debbagh, near Guelma Algeria' Town. After milling and sieving the ore in a fine powder, distilled water was

added to obtain a paste. This last was formed in cylindrical containers with their lids. One can note that no additive mater was used. And the containers hardness was enhanced with optimizing the two calcination steps of the elaboration process. Also, to avoid cracks formation during the heating treatment of the containers, these last were dried three days in air at room temperature (298 K). The first calcination was performed in a Carbolite furnace RHF 1600, at 1073 K, overnight, with a rate of heating of 10 deg/min. The second heating step was performed with a rate of heating of 5 deg/min until 1653 K, and a two hours isothermal step at this temperature, which was followed by a natural cooling inside the furnace until room temperature.

For the whole of the static tests, the monazite pellets were immersed in bidistilled water at 291 ± 3 K, with a volume ratio of 1/50. Measurements were made for a maximum period of three months. The kinetic of dissolution was performed following the Ce dissolution in the leachates. We choose this element because it is used as an An chemical analogue (An simulator). The speed of dissolution was followed by either a Panalytical MagixPro X-ray fluorescence (XRF) spectrometer or a UV Kontron Instrument Uvicom 930. Both spectrometers were first calibrated. The UV Ce absorption wavelength was identified in a previous study to be at 300 nm [41]. The used Ce standard solution used was an Aldrich cerium ICP/DCP standard solution of 9995 μg/mL.

The leachates Ce concentrations M (g/m^3) were deduced from the spectrometric calibration curves. The normalized leaching of Ce, RL (g/m^2), for each range of time, taken from the starting time of test, was calculated using the formula: $RL = MV_l/S_0W$, where V_l is the total volume of the leaching mixture (m^3), S_0 is the initial sample surface in contact with the leachate (m^2), and W is the weight fraction of Ce in the material. S_0 was assumed to be constant during the tests, and the initial Ce concentration in the leachate, negligible.

The Ce normalized dissolution rate RL (g/m^2 day) was deduced from the derivative values of the Ce normalized leaching. The Origin Pro 9 software was used for the mathematical calculations.

The microwave leach test was performed in an Ethos D microwave reactor, using the digestion/application note: DG-CE-01 for ceramic/refractory mixtures. This test is one of the most aggressive tests for the refractory ceramics (as corundum). The milled samples were immersed in a mixture of HNO_3-HCl-HF at 503 K at 1000 W for 15 and 20 min, successively. The monazite speed of dissolution was followed qualitatively and quantitatively by a Philips MagixPro X-ray fluorescence (XRF) spectrometer.

3. Results

The main physical characteristics of the monazite obtained by both the dry and wet syntheses routes are reported in Table 1.

The synthesis reactions yields are high values showing the applicability of the used methods. The sol–gel yield is lower than 80% due to CO_2, NO_2 and NO mass losses during the heat treatments. Both the green (d_g) and sintered (d_s) densities are comparable each other. The d_g densities are lower than those obtained by both Terra et al. and Montel et al. [28,42], which find a green density of 3.5 g/cm^3 with using a compacting pressure of 100 MPa in the fabrication process. One can explain this gap with the chemical composition of the phosphate, which contains heavier atoms compared to the present monazite chemical composition. The d_s densities are slightly lower than those found by the same cited authors, whose values increase with the sintering temperature (from 4.860 to 5.110 g/cm^3, for sintering temperatures in the range of 1623–1773 K). If one considers the sintering temperature of 1473 K, which is lower than 1623 K, our values are comparable to these last. The d_{rel} densities are good values (over 90%TD), showing a satisfactory densification of the sintered materials, obtained with both the wet and dry synthesis methods.

Table 1
Physical characterization of both the dry and wet routes made monazite.

Synthesis method	Sol–gel	Dry method
Reaction yield (%)	77	90
Morphological aspect	Light brown	Dark brown
d_g (±0.004 g/cm^3)	2.308	2.290
d_s (±0.004 g/cm^3)	4.700	4.550
d_{rel} (%TD)	97.73	94.32
Microstructure		
JCPDS[a] patterns after calcination at 873 K	00-032-0386 ($GdPO_4$)	01-084-0920 ($GdPO_4$)
JCPDS[a] patterns after sintering at 1473 K	01-083-0655 ($SmPO_4$) (94% monazite-type material) 01-076-1831 (6% monoclinic $Pb_2O_{3.33}$)	01-083-0655 ($SmPO_4$) (56% monazite-type material) 00-043-0469 (32% anorthic $Pb_2P_2O_7$) 01-049-8435 (12% anorthic $Ce_{11}O_{20}$)
Average grains size[b] (±0.05 μm)	4.34	3.89
Microhardeness (±5 HV)	298	232
Specific area (m^2/g)	0.707 ± 0.009	0.816 ± 0.003

[a] X'Pert High Score [40].
[b] Calculated for the main crystalline phase.

Typical diffractograms of the monazite for both the two used synthesis processes are given in Fig. 1. The main crystalline structure of the minerals is the monoclinic phase of the JCPDS standard data $Sm(PO_4)$ number 01-083-0655 for both the dry and wet route obtained monazites, respectively [40]. The skeletal of the monoclinic monazite is obtained since the first calcination at 873 K, for both routes of synthesis.

For the dry way monazite made, two secondary phases were identified: a lead phosphate $Pb_2P_2O_7$ and a lanthanides oxide phase in a typical form of $Ce_{11}O_{20}$, corresponding to the JCPDS data number 00-043-0469 and 01-049-8435, respectively [40]. In our material, this latter oxide may be substituted totally or partially with at least one of the lanthanides Gd, Ce or Y.

Bregiroux et al. [2] also report the formation of a $Ca_2P_2O_7$ secondary phase appearing with a plutonium monazite $(Pu^{3+}_{1-2x}Pu^{4+}_xCa^{2+}_x)PO_4$ synthesized in an oxidizing atmosphere of sintering below 1573 K.

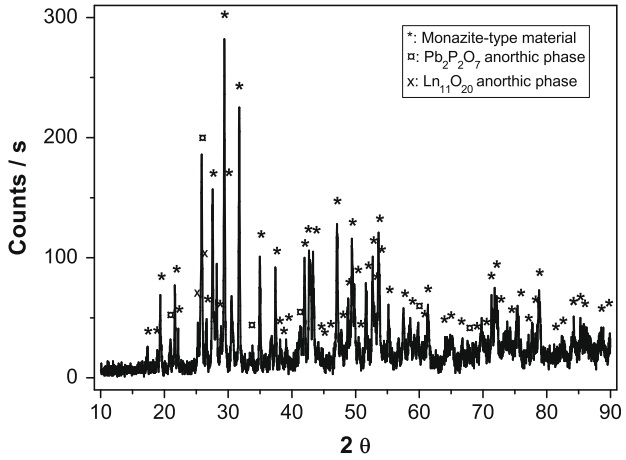

Fig. 1. Typical XRD spectra of the synthesized monazite. (a) Dry method. (b) Sol–gel method.

Few amounts (not exceeding 6 wt.%) of lead oxide $Pb_2O_{3.33}$ were identified in the wet route obtained monazite diffractogram (JCPDS data number 01-076-1831 [40]).

The SEM micrographs of the final sintered products are depicted on Figs. 2 and 3, for the dry route and sol–gel route made monazites, respectively.

On the monazite SEM pictures, the marked grains are the main monoclinic phase (elliptic mark) and the anorthic secondary phase (square mark). For the dry-route made monazite, the grains shape reflects the monoclinic and anorthic phase's forms showing a multi-phase material.

Thus, the sol–gel synthesis method gives a better monazite material than the dry route method.

These results are consistent with the results of the XRD analysis, and agree with those of the literature [43].

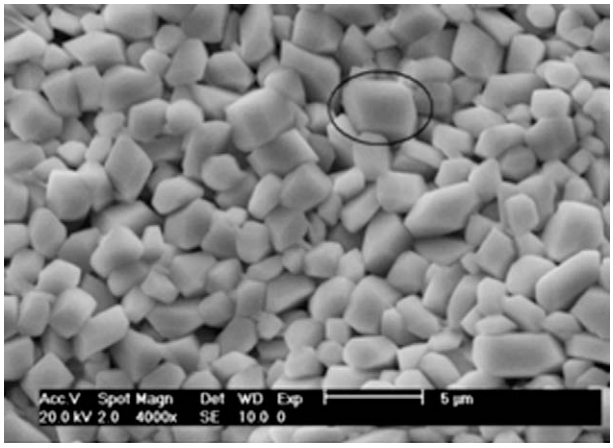

Fig. 2. Typical SEM micrograph of the dry-route made monazite. (a) The main monoclinic phase. (b) The anorthic secondary phase.

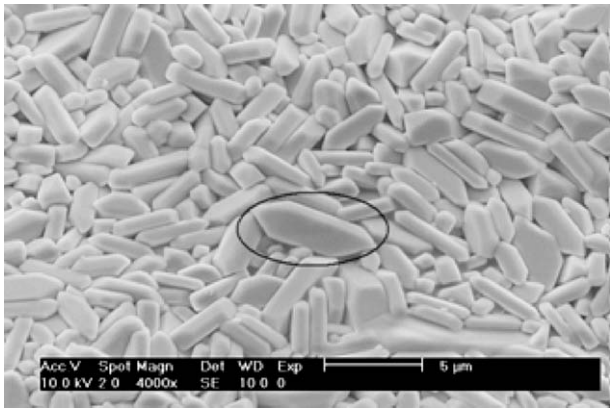

Fig. 3. Typical SEM micrograph of the sol–gel route made monazite.

Bregiroux et al. [34] have also reported that the solid-state synthesis of monazites containing several lanthanides, at temperatures lower than 1623 K, gave multiphase's materials.

The EDX analyses allow comparison between the expected monazite formula and the experimentally obtained monazite chemical formula. The results are summarized in Table 2. They corroborate the XRD analysis and confirm the successful synthesis processes of monazite. However, the secondary phases as the oxides $Pb_2O_{3.33}$ and $Ce_{11}O_{20}$ are not clearly evidenced on the micrographs and consequently the EDX analysis was not performed for these probably occurring residual compounds.

The minerals microhardnesses are high values. The microhardness is directly dependent on the lanthanides and other metallic dopents (Ca or Pb). Hernandez and Martin [44] prove that the P/Ce ratio strongly influence the hardness of the monazite. For P/Ce = 1.07, the monoclinic obtained form has a microhardeness of 173 HV for a 9.81 N charge. This value is slightly small than our values that are between 298 and 232 HV for a 30 N charge. One can attribute this difference to the used dopents, particularly Gd which is heavier than Ce and Pb.

Nevertheless, Perriere et al. [35] report indentations values (≈5 GPa) which are about five times higher than our values, for $LnPO_4$ monazites (Ln = La to Gd).

The specific areas are very low showing the less porous character of the synthesized monazite.

Montel et al. [42] report BET areas in the interval of 0.2–7.0 m^2/g, depending on the powders treatments.

The acidic leaching test was performed only on the sol–gel made monazite. However, the neutral pH static test was performed on the monazite made by the two ways of synthesis, but also in glass and kaolin containers in order to assess the efficiency of a storage kaolin medium for this kind of studied minerals.

The evolution of the Ce concentration in the leachates M (g/m^3) according to time t (day) gave the results gathered in Table 3. The variations according to time of the corresponding normalized dissolution rates RL are shown on Fig. 4 and 5.

For the whole of the leaching experiments, the Ce leached amounts decrease significantly after 30 days of tests. One can deduce that the kinetic of the leaching process is fast.

The evolution of the Ce normalized dissolution rate (RL) follows an exponential decay law for the acidic tests of pHs 1 and 4, (Table 4). For the other leaching experiments, the rapid decay of the amounts of leached Ce does not obey to any simple mathematical law.

For the sol–gel made monazite, the pH 1 leaching test gives higher extracted Ce amounts than the pH 4 leaching test. For pH 7 experiment, these amounts are also lower than these obtained for the pH 4 experiment. At the steady-state, the total amounts of Ce remaining in the leachates are about 5.668, 0.189 and 0.346×10^{-2} g/m^2 day, for pHs 1, 4 and 7 experiments, respectively.

If one compare the normalized dissolution rates in acidic conditions of leaching (pHs 1 and 4) to acceptable values for nuclear waste forms (which are about 10^{-3}–10^{-4} g/m^2 day for the actinides release from Synroc, leached by the MCC1 leaching procedure,

Table 2
Comparison between the theoretical and EDX-calculated chemical formula of the synthesized monazite.

Synthesis method	Sol–gel	Dry method
Expected formula	$(Y^{IV}_{0.1}Pb^{II}_{0.1}Ce^{III}_{0.4}Gd^{III}_{0.4})PO_4$	
Calculated formula	$(Y_{0.300}Pb_{0.017}Ce_{0.342}Gd_{0.341})P_{0.995}O_{4.129}$[a]	$(Y_{0.217}Pb_{0.143}Ce_{0.318}Gd_{0.322})P_{0.998}O_{4.032}$[a] $(Y_{0.147}Pb_{0.406}Ce_{0.222}Gd_{0.225})_2P_{1.663}O_{6.898}$[b]

[a] Monazite-type material main phase.
[b] Anorthic phosphate phase.

Table 3
Evolution of the Ce concentration in the leachates M (g/m^3), according to time t (day), for the static leaching tests.

Synthesis method	Sol–gel			Dry method		
Leaching method	Acidic method			In kaolin media[a]	Water static test[a]	In kaolin media[a]
pH[b]	1	4	7	≈7	≈7	≈7
pH[c]	≈1.6	≈2.5	≈5.5	≈5.3	≈5.5	≈5.3
t (day)	M (±0.003 g/m^3)					
0	0	0	0	0	0	0
1/4	–	–	–	5.620	–	2.966
1/2	2.573	1.400	0.058	–	–	–
1	6.452	5.927	0.070	3.100	–	2.533
2	–	–	–	3.115	1.112	3.976
3	17.638	3.326	0.890	3.335	0.982	3.420
6	19.687	4.048	4.759	–	–	–
7	–	–	–	5.188	5.879	16.009
8	26.192	8.919	0.309	–	–	–
9	–	–	–	2.035	8.336	9.883
10	–	–	–	2.141	7.767	7.540
13	29.195	9.165	0.263	1.358	13.767	5.992
15	25.139	8.434	0.174	1.338	–	–
16	–	–	–	1.338	13.523	5.024
20	28.874	10.538	0.109	–	–	–
23	20.095	7.495	0.981	–	–	–
27	17.955	9.702	0.884	–	–	–
29	–	–	–	1.247	10.255	10.411
30	5.864	8.625	–	–	–	–
34	5.860	5.614	0.855	1.208	7.439	8.118
38	5.850	4.612	0.854	1.077	6.218	7.241
42	5.848	3.820	0.850	–	6.512	5.584
45	5.847	3.820	0.848	–	6.014	5.210
48	5.847	3.820	0.845	–	5.845	4.662
49	5.847	3.820	0.845	0.766	–	–
55	5.847	3.820	0.845	0.770	4.924	4.021
62	5.847	3.820	0.845	0.770	4.875	3.024
69	5.847	3.820	0.845	0.770	4.210	2.228
76	5.847	3.820	0.845	0.770	3.981	2.147
83	5.847	3.820	0.845	0.770	3.248	0.729
90	5.847	3.820	0.845	0.770	1.842	0.687

[a] These values are deduced from UV measurements. The other data are measured by XRF analysis.
[b] These values are measured in the starting of the leaching tests.
[c] These values are measured at the end of the leaching tests.

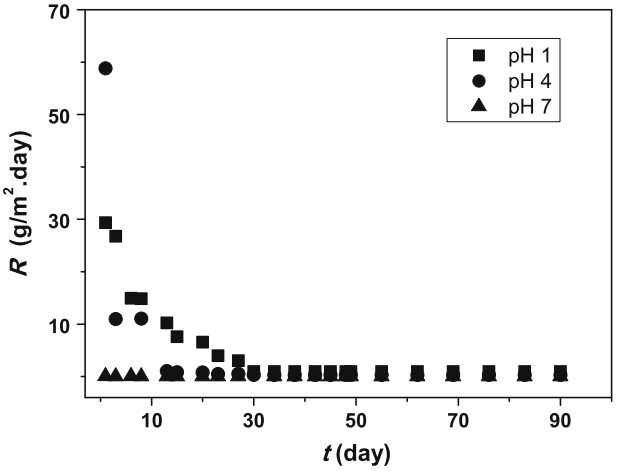

Fig. 4. Evolution of the Ce rate of leaching R (kg/m^2.s), according to time t (d), for the acidic leaching test.

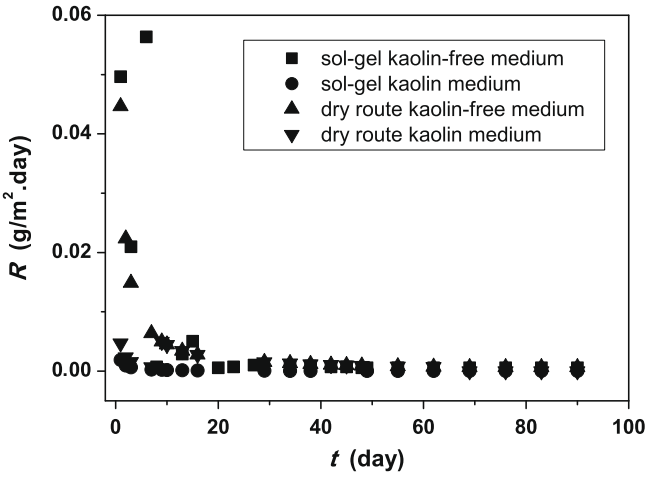

Fig. 5. Comparison of the Ce rate of leaching R (kg/m^2.s), according to time t (d) in both kaolin and kaolin-free leaching media.

and about 10^{-2} g/m^2 day for the vitrified waste forms [45]), the sol–gel made monazite has a weak chemical durability in acidic media (pHs 1 and 4). And it has an acceptable chemical durability in the neutral medium of leaching.

The observed weak chemical durability should be attributed in part to the employed synthesis process, particularly to the compaction/calcination steps, which may be improved.

In a neutral pH medium of leaching, both the sol–gel and the dry-route made monazites give comparable values of Ce rates of leaching (0.346×10^{-2} and 0.389×10^{-2} g/m^2 day, respectively). However, for both routes of synthesis, the leaching in kaolin media significantly (with a ten factor) decreases the amounts of leached Ce, which do not exceed 2.592×10^{-4} and 0.864×10^{-4} g/m^2 day for the wet and dry route obtained monazites, respectively. Thus, the kaolin leaching media inhibits the Ce dissolution. This is a good result, which leads us to expect the study of the possibility of use this monazite material in the case of a geological storage of nuclear waste.

In order to elucidate a correct understanding of the leaching phenomena and to explain the decrease of the amounts of leached Ce in the leachates, one can consider the formation of a lanthanides-bearing layer coating the surface of the leached samples.

Because of the lack of more accurate analytical methods, this was investigated by both the SEM-EDX and XRD analyses.

Table 4
The mathematical relations of the Ce normalized dissolution rate RL (g/m^2 day) versus time t (day), in acidic pH leaching conditions.

pH	1	4
RL = $f(t)$	RL = 193.343 · exp(−t/10.639)	RL = 786.227 · exp(−t/1.238)
Chi2*	67.379	308.176
R^{2**}	0.981	0.963

* Chi (χ) square.
** is the adjusted R-square.

In spite of the high amounts of the normalized dissolution rates, the SEM analysis of the leached samples gave the same microstructural features than those of the non-leached monazites, particularly for the acidic leaching tests (Fig. 6).

One can observe a deposited material (in dark) for the monazite material leached at pH 7. Both EDX and XRD X'Pert High Score analysis [40] conducts to the information's gathered in Table 5.

Because of the limits of the EDX analysis, the main results do not allow us to identify clearly the chemical composition of the leached materials altered surfaces. The atomic composition of the samples measured by EDX permit to reach the expected monazite chemical formula, by analyzing characteristic grains areas.

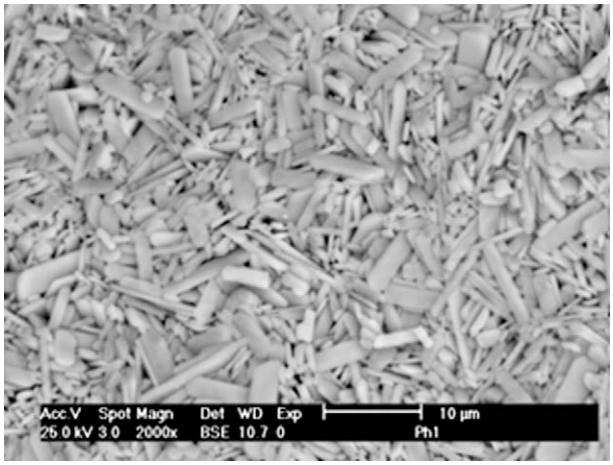

Fig. 6. SEM micrographs of the sol–gel made monazite leached in acidic conditions. (a) pH 1. (b) pH 4. (c) pH 7.

In the case of the leaching tests performed in the neutral leaching media, the coating layers of the matrices are multi-phase deposits (see XRD data of Table 6). Also, we were not able to identify by EDX analysis the accurate chemical formulas of each deposited compound.

One can remark the total dissolution of Pb in the samples leached in acidic pH conditions. One cannot confirm the same observation for the samples leached in neutral pH media, since we were not able to write the chemical formulas of the several compounds, which are present in the coating layer of the leached monazites.

Table 6
Leaching data of the microwave leaching test.

Synthesis method (%)	Sol–gel	Dry method
Rate of dissolved Ce	0.55	0.91
Microwave dissolution test		
Ratio of destroyed sample	3.5	4.0
Rate of dissolved Ce	8.14	7.98
Rate of dissolved Gd	Traces[a]	Traces[a]
Rate of dissolved Y	Traces	Traces
Rate of dissolved Pb	7.59	7.52
Rate of dissolved P	92.31	92.90

[a] Traces are amounts of elements undetectable by XRF analysis (<5 ppm).

The total dissolution of Pb leads to the formation of lanthanides (III) phosphates, free of Pb^{2+} bivalent cation, in which the lanthanides are all in the trivalent state. These phosphated compounds are probably Ln^{3+} rabdophane precipitates, as reported by Du Fou De Kerdaniel et al. [29]. The Ln^{3+} rabdophane precipitates are formed at low temperatures, and transform into monazite with a probable temperature raise. However, the precipitates bearing tetravalent cations tend to form phosphate hydrogen phosphate hydrate (PHPH) or rabdophane compounds, which transform again into PHPH phases.

Clavier et al. [33] report that in acid media, the lanthanides and thorium were quickly precipitated as neoformed phosphate-based

Table 5
EDX and XRD data of the leached surfaces for both the dry and sol–gel made monazite.

Analysed surface	Before leaching	After leaching
The sol–gel made monazite		
XRD data[a]		
Acidic leaching test	94% monazite-type material (JCPDS 01-083-0655)	pH 1 monazite-type material (JCPDS 01-083-0655)
	6% $Pb_2O_{3.33}$ (JCPDS 01-076-1831)	pH 4 monazite-type material (JCPDS 01-083-0655) pH 7 48% monazite-type material (JCPDS 01-083-0655) 28% $(Sm_2O_3)_{0.77}(La_2O_3)_{0.23}$ (JCPDS 01-077-2316) 24% LaP_3O_9 (JCPDS 01-084-1635)
EDX data		
Expected formula	$(Y^{IV}_{0.1}Pb^{II}_{0.1}Ce^{III}_{0.4}Gd^{III}_{0.4})PO_4$	–
Calculated formula	$(Y_{0.300}Pb_{0.017}Ce_{0.342}Gd_{0.341})P_{0.995}O_{4.129}$ of the main phase on the micrograph	pH 1 $(Y_{0.445}Ce_{0.351}Gd_{0.204})P_{0.995}O_{3.988}$[b] pH 4 $(Y_{0.457}Ce_{0.343}Gd_{0.200})P_{0.995}O_{3.988}$[b] pH 7 not determined[c]
The dry-route made monazite		
XRD data*		
Static leaching test	56% monazite-type material (JCPDS 01-083-0655) 32% anorthic $Pb_2P_2O_7$ (JCPDS 00-043-0469) 12% anorthic $Ce_{11}O_{20}$ (JCPDS 01-049-8435)	In kaolin media 10% anorthic $Ce_{11}O_{20}$ (JCPDS 01-049-8435) 15% LaP_3O_9 (JCPDS 01-084-1635) In glass media 75% monazite-type material (JCPDS 01-083-0655) 48% monazite-type material (JCPDS 01-083-0655) 28% $(Sm_2O_3)_{0.77}(La_2O_3)_{0.23}$ (JCPDS 01-077-2316) 24% LaP_3O_9 (JCPDS 01-084-1635)
EDX data		
Expected formula	$(Y^{IV}_{0.1}Pb^{II}_{0.1}Ce^{III}_{0.4}Gd^{III}_{0.4})PO_4$	–
Calculated formula	$(Y_{0.217}Pb_{0.143}Ce_{0.318}Gd_{0.322})P_{0.998}O_{4.032}$ of the monazite-type phase on the micrograph	In kaolin media Not determined[c]
	$(Y_{0.147}Pb_{0.406}Ce_{0.222}Gd_{0.225})_2P_{1.663}O_{6.898}$ of the secondary anorthic phosphate phase	In kaolin-free media Not determined[c]
	The lanthanides oxides $Ce_{11}O_{20}$ grains were not properly identified by SEM-EDX analysis	

[a] Determined by X'Pert High Score [40].
[b] The lanthanides are in the trivalent state in a phosphate matrix free of bivalent cations.
[c] Excess of O element do not allow calculating the probably occurring chemical formulas in a unknown multi-phase system.

phases (rabdophane or monazite for lanthanides). The presence of these phases could significantly delay the release of cations in the leachate.

In our study, the identified oxide phases (Table 5) are probably a consequence of the great solubility of Pb^{2+} in the leachates, which should induce the formation of these oxides (instead of rhabdophane or PHPH forms). The oxide deposits are probably in a hydrated form when the samples are still in the leachate media. And then they are dehydrated when the samples are removed out of the leachates for the purpose of the EDX/DRX investigations.

The great amounts of oxygen found on the samples surface for the materials leached in neutral pH conditions denote the strong probability of formation of some lanthanides phosphate and lanthanides oxides species. This results confirmed by XRD data necessitate full structural investigations with more accurate analytical techniques.

Bregiroux et al. [2,34] report the heterogeneous composition of a dry way monazite made containing several lanthanides. One can forecast in our case the presence of different compounds at the surface of the leached samples, because we used three lanthanides (Gd, Y, Ce). These compounds are not the result of the leaching process, but may also be present in the monazite structure it-self, as secondary phases, before leaching. Much more investigations must be performed to elucidate the exact composition of the coating layers of the presently studied monazite.

Veilly et al. [21] found normalized dissolution rates of 2.16×10^{-5} g/m^2 day in dynamic conditions of leaching and in an acid medium (≈pH 1, and 363 K). For the same experimental conditions, these aggressive leaching parameters lead to a better chemical durability of the monazite compared to that found for our samples (5.668 g/m^2 day). This good result may be attributed to the synthesis method; particularly the successive grinding/sintering steps improve the microstructure of the materials. Adding to that, this monazite contains Th which is known for tightening the microstructure, and then enhances the chemical durability of this synthesized monazite and other phosphate based matrices (thorium phosphates, britholites and pure cheralites). These matrices are coated with thorium phosphate barriers onto their surfaces when they are submitted to leaching tests [46,47].

However, in neutral pH leaching conditions and at room temperature, our results (8.64×10^{-6} and 8.64×10^{-7} g/m^2 day, respectively in kaolin-free and kaolin media) are in the same order of those given by these authors. Moreover, there are better to those for the dissolution of La from $LaPO_4$ at 369 K, which were quantified to 8.64×10^{-4} g/m^2 day by Bois et al. [48].

Terra et al. [28] also found better dissolution rates (between 8.64×10^{-7} and 8.64×10^{-4} g/m^2 day) compared to our acidic leaching media results for a La–Gd-bearing monazite synthesized by different methods, and leached in an acidic aggressive medium of leaching, in a temperature interval of: 291–363 K.

In another investigation, Terra et al. [30] report a rate of U dissolution in the order of 8.64×10^{-5} g/m^2 day, and have evidenced the formation of neoformed phases onto the materials surfaces. There results were confirmed by Du Fou de Kerdaniel et al. [29].

Oelkers and Poitrasson [24] and Poitrasson et al. [49] studied the dissolution of a natural monazite in a wide range of experimental conditions (323–503 K, and pH = 1–10) and found better dissolution rates compared to our results, namely: 5.97×10^{-7} to 4.48×10^{-4} g/m^2 day. They give full details on the solubility controlling phenomena for a neodymium phosphate phase. They prove the efficient immobilization of trivalent lanthanides (and then actinides) in a synthetic monazite.

The microwave leaching test was performed for both the dry and wet synthesis made monazite. The ratio of the destroyed mineral was determined by weighing the filtered and dried leached mineral sample. The leachates analysis gives the chemical composition, expressed in amounts of dissolved metals, shown in Table 6.

The distribution of the metals concentration in the leachates shows that Gd and Y are not present in the solutions. One can make the assumption that they were less soluble compared to Ce and Pb. These two last metals are however in week concentrations. The main solubilised metal is P.

The solubilisation of the minerals under a HNO_3–HCl–HF attack is partially achieved. The maximum amounts of released Ce did not exceed 0.55% and 0.91% for the sol–gel and dry-route made monazite, respectively; and only 3.5% and 4.0% of the mineral weight is solubilised from the sol–gel and dry-route made monazite, respectively.

Vettraino et al. [39] gave high amounts of destroyed samples of zirconia inert matrices (about 40–60%). Compared to these high values, one can deduce that the synthesized monazite is chemically very stable for the two ways of synthesis.

Regarding to the high amounts of dissolved P and Pb, one can conclude that this last test confirms the formation of deposited species free of P and Pb, appearing in the form of oxides on the surface of the materials analysed by XRD analysis.

Additional investigations must be performed to understand the relative solubility of these species and to elucidate the dissolution/precipitation mechanisms in this case.

4. Conclusions

A lanthanides phosphate containing lead with the chemical formula of $(Y_{0.1}Pb_{0.1}Ce_{0.4}Gd_{0.4})PO_4$ was synthesized by two methods: a sol–gel and a dry synthesis method. The Pb is added as a bivalent cation, and Ce simulates an actinide. In both syntheses, a supplementary calcination step at 873 K was added to eliminate the organic and nitride compounds. This leads to compact final products.

The synthesis reaction yields reach 77% and 90% for the sol–gel and dry route synthesis, respectively, showing the applicability of the used synthesis methods. The corresponding sintered densities are 4.70 and 4.55 g/cm^3 for a compacting pressure of 240 MPa. The relative densities, comprised between 90 and 95%TD, show a high capability of the studied material to sinter under the used synthesis conditions.

The determination of the physico-chemical properties of the synthesized monazite allow to assess the efficiency of the chosen fabrication processes.

The physical properties such as density, spectroscopic, and microscopic properties are satisfactory results.

The minerals main crystalline phase is a monazite-type material structure, for both the dry and wet route obtained monazites, respectively. The skeletal of a monoclinic monazite is obtained since the first calcination at 873 K for both routes of synthesis. For the dry way monazite made, two secondary phases were identified: a lead phosphate $Pb_2P_2O_7$ and a lanthanides oxide phase $Ln_{11}O_{20}$. Also, few amounts of lead oxide $Pb_2O_{3.33}$ were identified in the wet route obtained monazite.

One can conclude that the sol–gel synthesis method gives a better monazite material than the dry route method.

The minerals microhardnesses are high values ranging between 298 and 232 HV for a charge of 30 N. This result is a consequence of the monazite content in lanthanides and other metallic dopents (Pb). The BET specific surface areas are in the interval of 0.706–0.816 m^2/g, showing the less porous character of the monazite structure.

The bulk SEM-EDX determined atomic compositions in characterized areas (typically shaped) of the samples permit to reach the expected monazite chemical formula.

Since Ce is used as the actinide simulator, for the acidic water static leach tests at several pHs (1, 4 and 7), and for the long-term

geological disposal simulating conditions leach test (the kaolin test), we choose to follow the kinetic of the leaching with referring to the Ce dissolution according to time.

The acidic tests were performed only on the sol–gel made monazite; however the neutral pH static tests were performed on the monazite made by the two ways of synthesis, and either in glass or kaolin containers, in order to assess the efficiency of kaolin medium for the long-term storage of the studied actinides sequestration material.

For the whole of the leaching experiments, the kinetic of the leaching process is fast. For the sol–gel made monazite, the acidic tests gave few amounts of dissolved Ce. There are about 5.668, 0.189 and 0.346×10^{-2} g/m^2 day at the steady-state for the pH 1, 4 and 7 experiments, respectively. However, one can remark the total dissolution of Pb for the samples leached in acidic pHs (1 and 4).

One can conclude that the sol–gel made monazite has a weak chemical durability in acidic media. In the neutral medium of leaching, the sol–gel made monazite has an acceptable chemical durability.

For the leaching experiments in a neutral pH, both the sol–gel and the dry-route made monazites give comparable values of Ce normalized dissolution rates (0.346×10^{-2} and 0.389×10^{-2} g/m^2 day, respectively). The leaching in a kaolin medium decreases with a ten factor the amounts of leached Ce.

To elucidate a correct understanding of the diffusion phenomena and to explain the decrease of the leached Ce in the leachates, one can consider the formation of rabdophane –type compounds in the superficial layer coating the surface of the leached samples. This was investigated by both the SEM-EDX and XRD analyses of the leached samples surfaces. For acidic pH leaching experiments, XRD analysis gives only the monazite-type skeletal material with no additional coating material on the superficial layer. For the samples leached at pH 7, the XRD analysis revealed some multi-phase materials; and the EDX analysis shows an excess of oxygen element, which allow guessing an oxides lanthanides-bearing layer, coating the leached surfaces.

The XRD identified oxide phases are probably a consequence of the great solubility of Pb(II) in the leachates. These results should be confirmed with full structural investigations, with more accurate analytical techniques.

One can remark the total dissolution of Pb in the samples leached in acidic pHs conditions. One cannot confirm the same remark for the samples leached in neutral pH media.

For the acidic leaching tests, the total dissolution of Pb leads to the formation of lanthanides (III) phosphates, free of the Pb(II) bivalent cation, in which the lanthanides are all in the trivalent state. These phosphated compounds are probably Ln(III) rabdophane precipitates, which transform into monazite when the temperature increases.

The solubilisation of the minerals under the microwave leaching test is partially achieved. The maximum amounts of released Ce did not exceed 0.55% and 0.91% for the sol–gel and dry-route made monazite, respectively; and only 3.5% and 4.0% of the mineral are solubilised for the sol–gel and dry-route made monazite, respectively.

Regarding to the aggressiveness of the applied leaching test, one can make promising conclusions about the chemical durability of this Pb-containing monazite.

For both the sol–gel and the dry route of synthesis, one can deduce that the synthesized monazite is chemically stable in neutral media of leaching, but it is not chemically stable in acidic media. However, it is very resistant against dissolution under an aggressive microwave test.

One can conclude that the presently studied monazite should be more investigated to make valuable conclusions on the possibility of use this sequestration material as a potential candidate for the minor actinides confinement in kaolin geological undergrounds of nuclear waste storage.

Acknowledgements

We gratefully acknowledge the contribution of Nicolas Dacheux from Orsay Nuclear Physics Institute in France for the literature he provided us.

The authors also would like to thank Nassim Souami for the full investigation in SEM-EDEX analysis which was very usefull for the chemical identification of the mineral. We also acknowledge Mustapha Taouinet and Jahid Sahel for the mechanical characterization and SEM observations.

References

[1] J.M. Montel, J.L. Devidal, D. Avignant, Chem. Geol. 191 (2002) 89–104.
[2] D. Bregiroux, R. Belin, P. Valenza, F. Audubert, D. Bernache-Assollant, J. Nucl. Mater. 366 (2007) 52–57.
[3] K.L. Kelly, G.W. Beall, J.P. Young, L.A. Boatner, Valence states of actinides in synthetic monazites, in: J.G. Moore (Ed.), Scientific Basis for Nuclear Waste Management III, Plenum Publishing Corp, New York, 1981, pp. 189–195.
[4] N. Dacheux, R. Podor, B. Chassigneux, V. Brandel, M. Genet, J. Alloys Compd. 271–273 (1998) 236–239.
[5] C.M. Gramaccioli, T.V. Segalstrad, Am. Mineral. 63 (1978) 757–761.
[6] P. Pascal, Monazite. Nouveau traité de chimie minérale, Masson et Cie, Paris, 1956.
[7] L.A. Boatner, Rev. Mineral. Chem. 48 (2002) 87–121.
[8] W.O. Milligan, D.F. Mullica, G.W. Beall, L.A. Boatner, Inorg. Chim. Acta. 70 (1983) 133–136.
[9] R. Podor, M. Cuney, Am. Mineral. 82 (1997) 765–771.
[10] T.W. Cheng, Mineral. Eng. 13 (2000) 105–109.
[11] K. Linthout, Can. Mineral. 45 (2007) 503–508.
[12] S. Lucas, Synthèse et comportement thermique (stabilité et frittage) de phosphates de terres rares cériques ou yttriques. Ph.D. thesis, Université de Limoges, 2003.
[13] F. Poitrasson, S. Chenery, D.J. Bland, Earth. Planet. Sci. Lett. 145 (1996) 79–96.
[14] W. Miller, R. Alexander, N. Chapman, I. McKinley, J. Smellie, Geological Disposal of Radioactive Wastes and Natural Analogues, Pergamon Press, New York, 2000.
[15] R.C. Ewing, Can. Mineral. 39 (2001) 697–715.
[16] R.C. Ewing, Earth. Planet. Sci. Lett. 229 (2005) 165–181.
[17] E.C. Gaucher, P. Blanc, Natural analogues, and modeling, Waste Manage. 26 (2006) 776–788.
[18] H.J. Forster, Lithos 88 (2006) 35–55.
[19] N.T. Rempe, Prog. Nucl. Energy. 49 (2007) 365–374.
[20] F.G.F. Gibb, K.J. Taylor, B.E. Burakov, Mater. Res. Soc. Symp. Proc. 1107 (2008) 51–58.
[21] E. Veilly, E. Du Fou de Kerdaniel, J. Roques, N. Dacheux, N. Clavier, Inorg. Chem. 47 (2008) 10971–10979.
[22] L. Campayo, F. Audubert, D. Bernache-Assolant, Sol. Stat. Ion. 176 (2005) 2663–2669.
[23] E. Gardes, O. Jaoul, J.M. Montel, Geochim. Cosmochim. Acta. 70 (2006) 2325–2336.
[24] E.H. Oelkers, F. Poitrasson, Chem. Geol. 191 (2002) 73–87.
[25] L.A. Boatner, in: M.L. Kohn, J. Rakovan, J.M. Hughes (Eds.), Phosphates: Geochemical, Geobiological and Materials Importance, Mineralogical Society of America, Washington, DC, 2002, pp. 87–121.
[26] D.J. Cherniak, J.M. Pyle, Chem. Geol. 256 (2008) 52–61.
[27] K. Popa, D. Sedmidubsky, O. Benes, C. Thiriet, R.J.M. Konings, J. Chem. Thermodyn. 38 (2006) 825–829.
[28] O. Terra, N. Clavier, N. Dacheux, R. Podor, New J. Chem. 27 (2003) 957–967.
[29] E. Du Fou de Kerdaniel, N. Clavier, N. Dacheux, O. Terra, R. Podor, J. Nucl. Mater. 362 (2007) 451–458.
[30] O. Terra, N. Dacheux, F. Audubert, R. Podor, J. Nucl. Mater. 352 (2006) 224–232.
[31] O. Terra, N. Dacheux, N. Clavier, R. Podor, F. Audubert, J. Am. Ceram. Soc. 91 (2008) 3673–3682.
[32] N. Dacheux, N. Clavier, A.C. Robisson, O. Terra, F. Audubert, J.E. Lartigue, C. Guy, CR Chim. 7 (2004) 1141–1152.
[33] N. Clavier, N. Dacheux, R. Podor, Inorg. Chem. 45 (2006) 220–229.
[34] D. Bregiroux, O. Terra, F. Audubert, N. Dacheux, V. Serin, R. Podor, D. Bernache-Assollant, Inorg. Chem. 46 (2007) 10372–10382.
[35] L. Perrière, D. Bregiroux, B. Naitali, F. Audubert, E. Champion, D.S. Smith, D. Bernache-Assolant, J. Eur. Ceram. Soc. 27 (2007) 3207–3213.
[36] S.J. Patwe, A.K. Tyagi, Ceram. Int. 32 (2006) 545–548.
[37] O. Terra, F. Audubert, N. Dacheux, C. Guy, R. Podor, J. Nucl. Mater. 354 (2006) 49–65.
[38] O. Terra, F. Audubert, N. Dacheux, C. Guy, R. Podor, J. Nucl. Mater. 366 (2007) 70–86.
[39] F. Vettraino, G. Magnani, J. Nucl. Mater. 274 (1999) 23–33.

[40] Philips X'Pert High Score Package, Diffraction Data CD-ROM, International Center for Diffraction Data, Newtown Square, PA, 2004.
[41] N. Kamel, H. A-Amar, M. Taouinet, C. Benazzouz, Z. Kamel, H. Fodil-Cherif, S. Telmoune, R. Slimani, A. Zahri, D. Sahel, Prog. Nucl. Energy 48 (2006) 70–84.
[42] J.M. Montel, B. Glorieux, A.M. Seydoux-Guillaume, R. Wirth, J. Phys. Chem. Solids 67 (2006) 2489–2500.
[43] S.V. Ushakov, K.B. Helean, A. Navrotsky, L.A. Boatner, J. Mater. Res. 16 (2001) 2623–2633.
[44] T. Hernandez, P. Martın, J. Alloys Compd. 466 (2008) 568–575.
[45] W.E. Lee, M.I. Ojovan, M.C. Stennett, N.C. Hyatt, Adv. Appl. Ceram. 105 (2006) 3–12.
[46] N. Dacheux, N. Clavier, J. Ritt, J. Nucl. Mater. 349 (2006) 291–303.
[47] N. Clavier, J. Nucl. Mater. 349 (2006) 304–316.
[48] L. Bois, M.J. Guittet, F. Carrot, P. Trocellier, M. Gautier-Soyer, J. Nucl. Mater. 297 (2001) 129–137.
[49] F. Poitrasson, E. Oelkers, J. Schott, J.M. Montel, Geochim. Cosmochim. Acta. 68 (2004) 2207–2221.